



INTERNATIONAL SYMPOSIUM: WAVES - PHYSICAL AND NUMERICAL MODELLING

UNIVERSITY OF BRITISH COLUMBIA,
VANCOUVER, CANADA

AUGUST 21 - 24, 1994

NUMERICAL SIMULATION OF NONLINEAR DIRECTIONAL WAVES

BY AN IMPROVED BOUSSINESQ MODEL

Serdar Beji

Faculty of Naval Architecture and Marine Technology,
Istanbul Technical University, Maslak 80626, Istanbul, Turkey

and

Kazuo Nadaoka

Department of Civil Engineering, Tokyo Institute of Technology,
2-12-1 O-okayama, Meguro-ku, Tokyo 152, Japan

ABSTRACT

A numerical scheme for an improved Boussinesq model is developed for simulation of nonlinear, short-crested wave transformations over slowly varying depths. The governing equations are discretized by three-time level finite-difference approximations to achieve an accurate treatment of the nonlinear terms. A higher order radiation condition is implemented for effective absorption of the outgoing waves. Ring test and wave propagation over a topographical lens are included as sample computations demonstrating the performance of the model.

INTRODUCTION

Due to strong interactions with bottom topography, waves observed in the surf zone are almost always nonlinear, and as it is obvious from the frequent occurrence of white-capping and breaking, nonlinearity is usually quite high. Any realistic modeling of these waves must therefore account for the nonlinear interactions, just as it must consider the eventually dissipative role of breaking.

At present weakly-nonlinear weakly-dispersive wave models, namely the Boussinesq type models, appear to be the most promising ones for practical applications. These depth-integrated equations at once reduce a three-dimensional problem to the solution of an equivalent (within the approximations made) two-dimensional problem. Such a reduction in dimension provides significant savings in computation time as well as a certain robustness originating from the simplified numerical procedure.

Despite these advantages the classical Boussinesq equations suffer from the inherent disadvantage of being shallow water equations. To extend their applicable range numerous attempts have been made (see the references in Nwogu, 1993). Here we shall use one such an improved model due to Beji and Nadaoka (1994), which might be viewed as a rectified version of Madsen and Sørensen's (1992) work. Accordingly, the dispersion characteristics of the present model are improved to the extent that waves with wavelengths equal to depth may be represented with acceptable errors in amplitude and celerity. However, for a varying depth the linear shoaling is accurate only if the depth to wavelength ratio at the incoming boundary is less than $\frac{1}{4}$, as demonstrated by Beji and Nadaoka (1994).

The governing equations are discretized by a three-time-level finite-difference approach so that the nonlinear terms could be treated as quasi-linear contributions. The second order radiation condition of Engquist and Majda (1977) is implemented for a better absorption of the directional waves and found to be quite satisfactory.

GOVERNING EQUATIONS

The improved Boussinesq equations of Beji and Nadaoka (1994) are chosen as the wave propagation model. The derivation procedure and details about the dispersion and linear shoaling properties of these equations can be found in this particular reference. The continuity and momentum equations are

$$\eta_t + \nabla \cdot [(h + \eta) \mathbf{q}] = 0, \quad (1)$$

$$\begin{aligned} \mathbf{q}_t + (\mathbf{q} \cdot \nabla) \mathbf{q} + g \nabla \eta = & (1 + \beta) \frac{h}{2} \nabla [\nabla \cdot (h \mathbf{q}_t)] + \beta \frac{gh}{2} \nabla [\nabla \cdot (h \nabla \eta)] \\ & - (1 + \beta) \frac{h^2}{6} \nabla (\nabla \cdot \mathbf{q}_t) - \beta \frac{gh^2}{6} \nabla (\nabla \cdot \nabla \eta), \end{aligned} \quad (2)$$

where $\mathbf{q}=(u,v)$ is the two-dimensional depth-averaged velocity vector, η is the surface displacement, $h=h(x,y)$ is the varying water depth as measured from the still water level, g is the gravitational acceleration, and β is a constant. The subscript t stands for partial differentiation with respect to time and ∇ for the horizontal gradient operator. The z -axis is taken vertically upwards with the origin at the undisturbed free surface.

In linearized forms equations (1) and (2) lead to the following dispersion relation

$$\frac{c^2}{gh} = \frac{(1 + \beta k^2 h^2 / 3)}{[1 + (1 + \beta) k^2 h^2 / 3]}, \quad (3)$$

where $c=|c|$ is the phase speed, $k^2=k_x^2+k_y^2$ and k_x, k_y are the components of wave-number vector k in the x - and y -directions respectively.

Matching equation (3) with a first-order Padé expansion of the linear theory dispersion relation requires $\beta=0$, which in turn reduces equation (3) to the classical Boussinesq dispersion relation. On the other hand, an expansion correct to the second-order dictates $\beta=1/5$, and naturally results in better agreement with the exact form of the linear theory dispersion relation. Here, $\beta=1/5$ is used in all computations.

In this connection it is worthy of remark that quite recently Nwogu (1993) has introduced an alternative procedure to improve the dispersion characteristics of the Boussinesq type equations. These equations, though different in form from (1) and (2), by choice may have the same linear dispersion curve. Their numerical solution for several cases was found to produce almost identical results with those of (1) and (2); however the non-conservation form of the continuity equation required special handling (specifically, it had to be discretized in a pseudo-conservation form) for obtaining accurate results. This approach however was not trouble-free and brought problems in the immediate vicinity of the boundaries.

BOUNDARY AND INITIAL CONDITIONS

Boundary Conditions

Boundary conditions at the rigid impermeable bottom and the free surface are automatically satisfied by the governing equations. It then remains to specify the conditions at the boundaries vertically enclosing the physical domain of interest. Boundaries along which incident waves are introduced are quite easy to deal with. Simply, velocity components and the corresponding surface displacement as computed from the continuity equation are specified (or vice versa). If the waves maintain a constant phase speed c , one can easily derive the following exact analytical expression from equation (1):

$$\eta = \frac{h(\mathbf{q} \cdot \mathbf{d})}{(c - \mathbf{q} \cdot \mathbf{d})}, \quad (4)$$

where \mathbf{d} is the direction vector with components $(\cos\theta, \sin\theta)$. Here θ is the angle between the wave propagation direction and the positive x -axis.

Besides the incoming boundary condition, two boundary conditions are of particular interest; namely, radiation condition and reflection condition. The latter does not pose any serious problems whereas the former demands special care and is often the most troublesome part of a numerical model.

A perfectly absorbing boundary condition for waves approaching at an oblique angle to a boundary would be

$$\mathbf{q}_t + (\mathbf{c} \cdot \nabla) \mathbf{q} = 0, \quad (5)$$

which implies that the velocity field is convected away at the constant phase celerity $|\mathbf{c}| = (c_x^2 + c_y^2)^{1/2}$ with $c_x = c \cos \theta$, $c_y = c \sin \theta$ being the components of the wave-celerity vector \mathbf{c} in the x- and y-directions respectively. However, the implementation of (5) is not trivial as it is a non-local boundary condition; that is, it requires information (the incident wave angle) from the interior points of the computational domain. In general it is quite difficult to compute the outgoing wave angle and the accuracy is not ascertained. It is therefore preferable to have a local boundary condition which does not require extra information from the interior points but has the capability of absorbing the obliquely incident waves with minimum reflection. To this end we refer to Engquist and Majda (1977) who introduced a systematic approach which can produce successively higher order absorbing boundary conditions. For a non-dispersive wave equation $w_{tt} - w_{xx} - w_{yy} = 0$ (here w represents either velocity or surface displacement) their first-order approach leads to the well-known Sommerfeld radiation condition which is appropriate for normally impinging waves. The second-order approximation on the other hand produces the following formula for waves traveling in the positive x-direction.

$$w_{tt} + w_{xt} - \frac{1}{2} w_{yy} = 0. \quad (6)$$

At the lowest order, when combined with (1), equation (2) is equivalent to the non-dispersive wave equation with a wave propagation celerity $c = \sqrt{gh}$. It is then a plausible approximation to use the dimensional form of equation (6) with the celerity $c = \sqrt{gh}$ as the radiation condition in solving equation (2). Thus, for waves propagating in the positive x-direction with the phase celerity c we employ the following radiation condition for the x-component of the velocity $q(u, v)$:

$$u_{tt} + c u_{xt} - \frac{1}{2} c^2 u_{yy} = 0. \quad (7)$$

If the waves are moving in the negative x-direction the sign in front of the second term reverses. The expressions corresponding to the y-component of the velocity are analogous.

Initial Condition

All computations are started by specifying u , v , and η over the entire domain for the first two time levels. Except for the ring test which is presented later as an example, the initial condition is the state of rest; that is, both the velocity field and the surface displacement are zero throughout the domain.

DISCRETIZATION

Discretization of Governing Equations

Beginning with the remarkable contribution of Peregrine (1967) the works on the finite-difference modeling of the Boussinesq equations appear to adhere to the two-time-level approach (Abbott *et. al.*, 1973, Schaper and Zielke, 1984, Madsen and Sørensen, 1992, Beji and Battjes, 1993). The main problem in these models is the accurate treatment of the nonlinear terms, which are to be evaluated at the mid-time level if the scheme be fully centered (see Abbott *et. al.*, 1984 for a detailed exposition). For the improved type Boussinesq equations the problem is augmented as extra terms proportional to the spatial derivatives of the surface displacement come into picture. Like the nonlinear terms these linear dispersion terms must be evaluated at the mid-time level as well.

A straightforward alternative to bypass all these difficulties presents itself as a three-time-level formulation. The original idea probably dates back from Zabusky and Kruskal's (1965) well-known work on the KdV equation. In a three-time-level formulation no special care is needed for the mid-time level values since they are known as an essential part of the entire process. The only burden comes from keeping the third-time-level values in memory, which is a rather small price for the accuracy and computational speed gained. For the reasons indicated a three-time-level approach is employed here; both space and time derivatives are centered and η , u , v are all placed at the same grid points, according to the pure leap-frog method.

To reduce the computational effort the solution process is decoupled so that only one variable is solved along each row or column until the entire domain is covered. Accordingly, the x-momentum equation is solved for u , the y-momentum equation for v . Such artificial decoupling of course necessitates some approximations and these are indicated below. Continuity equation does not require any additional approximation as it is possible to implement a simple explicit discretization. For brevity, only time derivatives are given in discretized forms. All spatial derivatives are approximated by central difference formulations. The x-sweep equation is

$$\begin{aligned}
 & \frac{(u^{k+1} - u^{k-1}))}{2\Delta t} - (1+\beta) \left[\frac{h^2}{3} \frac{(u_{xx}^{k+1} - u_{xx}^{k-1}))}{2\Delta t} + hh_x \frac{(u_x^{k+1} - u_x^{k-1}))}{2\Delta t} \right] \\
 & = -g\eta_x^k - \frac{1}{2} (u^2 + v^2)_x^k + (1+\beta) \frac{h^2}{3} \frac{(v_{xy}^{k+1} - v_{xy}^{k-1}))}{2\Delta t} \\
 & + \frac{1}{2} (1+\beta) \left[hh_x \frac{(v_y^{k+1} - v_y^{k-1}))}{2\Delta t} + hh_y \frac{(v_x^{k+1} - v_x^{k-1}))}{2\Delta t} \right] \\
 & + \beta g \frac{h^2}{3} (\eta_{xxx}^k + \eta_{xyy}^k) + \beta gh \left(h_x \eta_{xx}^k + \frac{1}{2} h_y \eta_{xy}^k + \frac{1}{2} h_x \eta_{yy}^k \right)
 \end{aligned} \tag{8}$$

in which the superscript k denotes the time level. Note that to improve the computational accuracy the nonlinear terms are re-expressed by using the

irrotationality condition $u_y = v_x^*$. The new time level values of v appearing on the right-hand side of (11) are treated as known by using the last computed values so that u^{k+1} 's are the only unknowns. The resulting matrix equation is tridiagonal and can be solved very efficiently by the Thomas algorithm (see Huyakorn and Pinder, 1983). Similarly the y -sweep is

$$\begin{aligned} & \frac{(v^{k+1} - v^{k-1})}{2\Delta t} - (1 + \beta) \left[\frac{h^2}{3} \frac{(v_{yy}^{k+1} - v_{yy}^{k-1})}{2\Delta t} + hh_y \frac{(v_y^{k+1} - v_y^{k-1})}{2\Delta t} \right] \\ & = -g\eta_y^k - \frac{1}{2} (u^2 + v^2)_y^k + (1 + \beta) \frac{h^2}{3} \frac{(u_{xy}^{k+1} - u_{xy}^{k-1})}{2\Delta t} \\ & + \frac{1}{2} (1 + \beta) \left[hh_y \frac{(u_x^{k+1} - u_x^{k-1})}{2\Delta t} + hh_x \frac{(u_y^{k+1} - u_y^{k-1})}{2\Delta t} \right] \\ & + \beta g \frac{h^2}{3} (\eta_{yyy}^k + \eta_{kxy}^k) + \beta gh (h_y \eta_{yy}^k + \frac{1}{2} h_x \eta_{xy}^k + \frac{1}{2} h_y \eta_{xx}^k) \end{aligned} \quad (9)$$

in which v^{k+1} 's are the only unknowns. The u^{k+1} 's and subsequently v^{k+1} 's obtained from respectively (8) and (9) are of course only a first estimate since these variables are computed separately. It is therefore necessary to iterate to obtain accurate results. For the computational tests presented later a single iteration was found to be sufficient but more complicated problems may require two iterations.

The surface displacement is obtained from a simple explicit discretization of the continuity equation:

$$\frac{(\eta^{k+1} - \eta^{k-1})}{2\Delta t} + [(h + \eta)u]_x^k + [(h + \eta)v]_y^k = 0. \quad (10)$$

Discretization of Radiation Condition

Equation (7) is discretized as central differences in time and backward differences in space:

$$\begin{aligned} & \frac{(u_{i,j}^{k+1} - 2u_{i,j}^k + u_{i,j}^{k-1}))}{\Delta t^2} + c \frac{(u_{i,j}^{k+1} - u_{i-1,j}^{k+1}) - (u_{i,j}^{k-1} - u_{i-1,j}^{k-1})}{2\Delta x \Delta t} \\ & - \frac{1}{2} c^2 \frac{(u_{i,j+1}^k - 2u_{i,j}^k + u_{i,j-1}^k)}{\Delta y^2} = 0 \quad \text{for } i = n, \end{aligned} \quad (11)$$

where i and j label the spatial points in the x - y Cartesian system. Note that equation (11) is valid for waves propagating in the positive x -direction. For waves moving in the negative x -direction and the y -direction the discretization procedure is completely analogous and is not repeated.

*Strictly speaking this is not valid for a varying depth but an acceptable approximation. See Peregrine (1967).

NUMERICAL SIMULATIONS

The performance of the numerical scheme described above is now illustrated for two selected cases. The first case is the ring test with a two-fold purpose. The first is to check the symmetrical accuracy of the numerical model and the second is to compare the first and second-order radiation conditions. A surface elevation of solitary-wave shape is initially imposed and then the computation is let to proceed on its due course. The initial wave height to depth ratio is 0.3. The computational area is $2\text{m} \times 2\text{m}$, which is discretized by 50 points along both x - and y -axes. The time step is $1/25$ second. The left column in Figure 1 shows the computational results with the first-order boundary condition at $t = \frac{1}{2}$, 1, and 2 seconds respectively. On the right column the corresponding results with the second-order boundary condition are depicted. As it is obvious from the surface profiles at $t = 2$ seconds the first order boundary condition is inferior, especially at the corners of the computational domain where the radiating wave angle is sharpest.

The second case is the computation of wave convergence over a bottom topography that acts as a focusing lens (Whalin, 1971). This test serves as a check on the performance of the numerical scheme itself in handling a complicated bathymetry and has been used frequently (see for instance Liu *et. al.*, 1985). Figure 2a shows a perspective view of the wave field. Figure 2b compares the computed harmonic amplitudes with the measured data (reproduced from the work of Madsen and Sørensen, 1992) along the centerline of the wave tank. The computation was performed with $\Delta x = \Delta y = \lambda_0/50$ m (λ_0 is the wavelength at the incoming boundary) and $\Delta t = T/50$ second, which rendered the initial Courant number unity. The incident wave period is $T = 2$ seconds.

CONCLUDING REMARKS

The performance of the numerical model appears to be good both in terms of accuracy and computational time. Use of the three-time-level formulation not only makes it possible to treat the nonlinear terms in the most straightforward manner but also shortens the computational time considerably by permitting an explicit formulation of the continuity equation as completely decoupled from the momentum equations. It must be indicated however that these advantages are purchased at the expense of additional storage necessary to keep the third time level values in memory.

Absorption of the outgoing waves that approach in multitude of directions is a delicate problem. The higher order radiation condition used here, as demonstrated by the ring test, is found to be reliable even in simulations with acute angles of wave radiation.

Since the merits of a numerical model cannot be judged without testing against field data, the eventual approval or disapproval of this model awaits such comparisons.

ACKNOWLEDGEMENT

This work was carried out while the first author was at T.I.T. through a grant from the Kajima Foundation of Japan and subsequently from T.I.T.

REFERENCES

- Abbott, M.B., A. Damsgaard and G.S. Rodenhuis (1973). System 21, "Jupiter" (A Design System for Two-Dimensional Nearly Horizontal Flows). *J. of Hydraulic Res.*, 11 (1), 1-28.
- Abbott, M.B., A.D. McCowan and I.R. Warren (1984). Accuracy of short-wave numerical models." *J. of Hydraulic Eng.*, 110-10, 1287-1301.
- Beji, S. and J.A. Battjes (1993). Numerical simulation of nonlinear wave propagation over a bar. *To appear in Coastal Eng.*
- Beji, S. and K. Nadaoka (1994). A formal derivation and numerical modeling of the improved Boussinesq equations for varying depth. *Submitted to Coastal Eng.*
- Engquist, B. and A. Majda (1977). Absorbing boundary conditions for the numerical simulation of waves. *Math. Comp.*, 31-139, 629-651.
- Huyakorn, P.S. and G.F. Pinder (1983). *Computational methods in subsurface flow*, Academic Press, New York.
- Liu, P.L.-F., S.B. Yoon and J.T. Kirby (1985). Nonlinear refraction-diffraction of waves in shallow water. *J. Fluid Mech.*, 153, 185-201.
- Madsen, P.A. and O.R. Sørensen (1992). A new form of the Boussinesq equations with improved linear dispersion characteristics. Part 2: A slowly-varying bathymetry. *Coastal Eng.*, 18, 183-204.
- Nwogu, O. (1993). Alternative form of Boussinesq equations for nearshore wave propagation. *J. Waterway, Port, Coastal, and Ocean Eng.*, 119-6, 618-638.
- Peregrine, D.H. (1967). Long waves on a beach. *J. Fluid Mech.*, 27, 815-827.
- Schaper, H. and W. Zielke (1984). A numerical solution of Boussinesq type wave equations. *Proc. 19th ICCE*, 1057-1072.
- Whalin, R.W. (1971). The limit of applicability of linear wave refraction theory in a convergence zone. *Res. Rep. H-71-3, U.S. Army Corps of Engrs, Waterways Expt. Station, Vicksburg, M.S.*
- Zabusky, N.J. and M.D. Kruskal (1965). Interaction of solitons in a collisionless plasma and recurrence of initial states. *Phy. Rev. Lett.*, 15, 240.

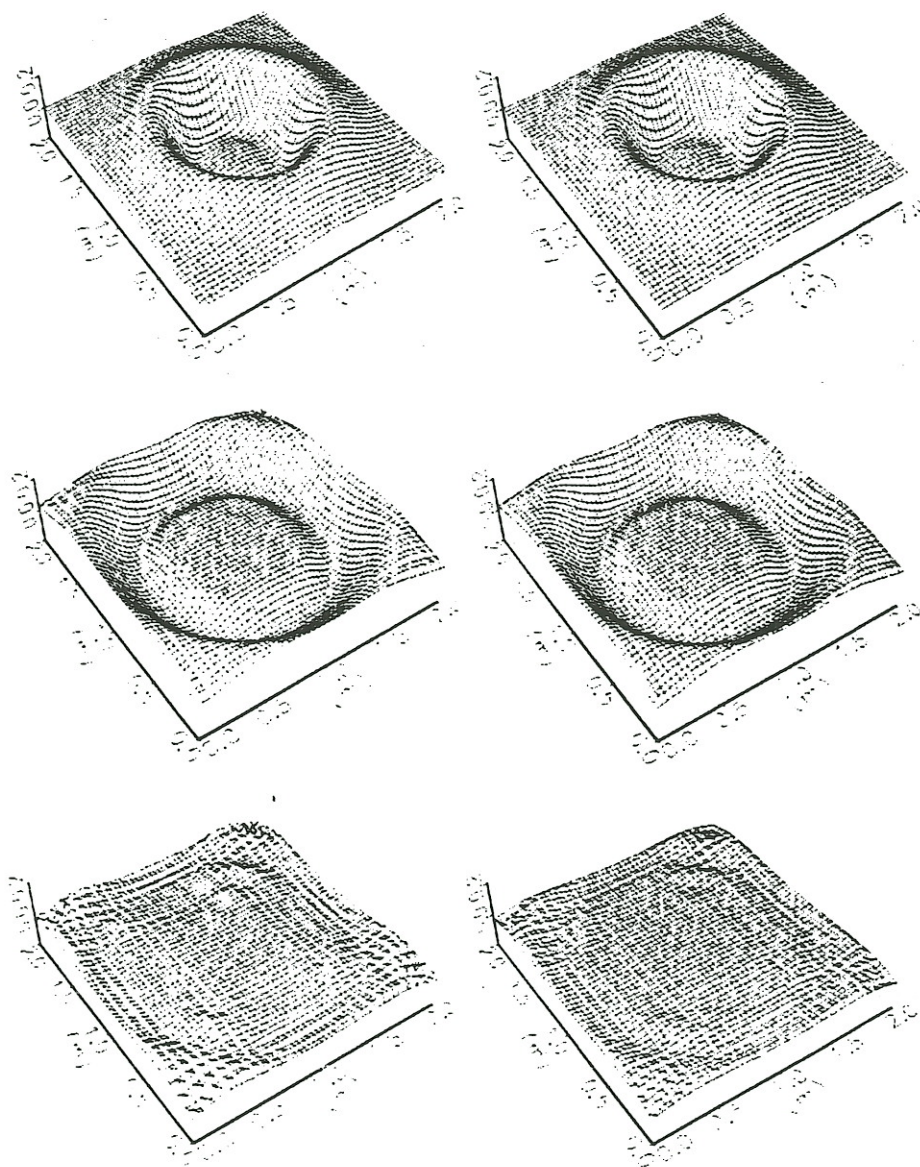


Figure 1 : Ring test displayed at $t=\frac{1}{2}, 1, 2$ seconds
 Left column: the first order radiation condition
 Right column: the second order radiation condition

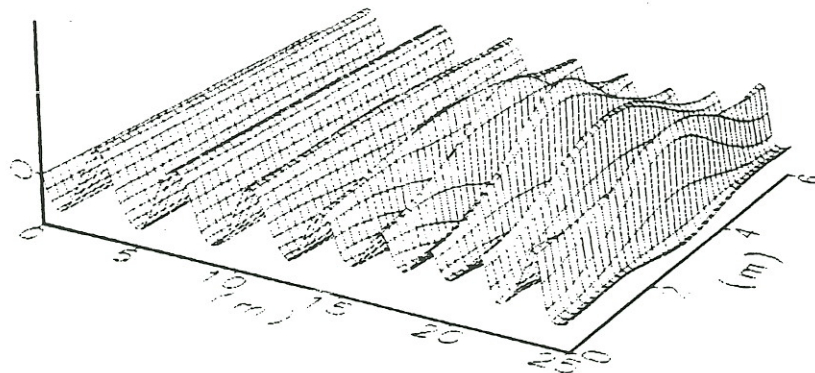


Figure 2a: A perspective view of the wave field

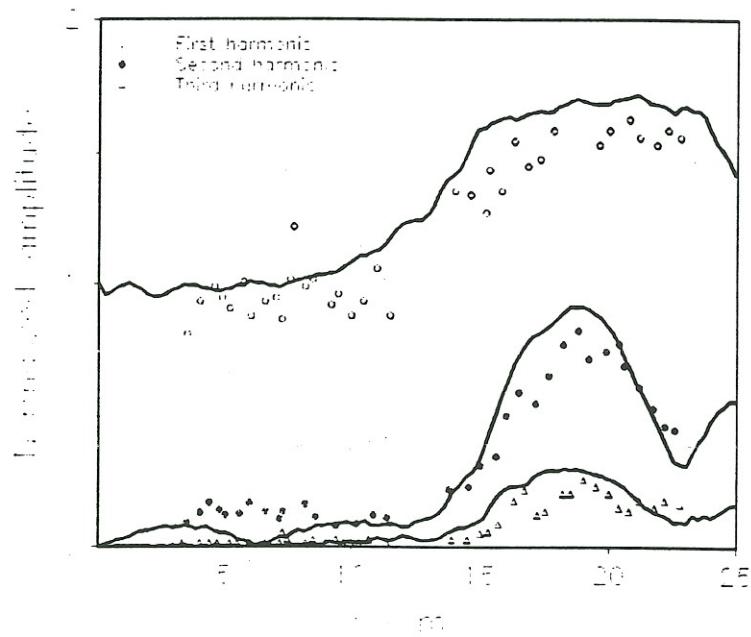


Figure 2b: Variation of the harmonic amplitudes along the centerline
Solid lines: computation, scatter: experimental data